Cellulose (2018) 25:2217–2234
https://doi.org/10.1007/s10570-018-1740-4

ORIGINAL PAPER

Dependence of dissolution, dispersion, and aggregation characteristics of cationic polysaccharides made from euglenoid β-1,3-glucan on degree of substitution

Motonari Shibakami · Tadashi Nemoto · Mitsugu Sohma

Received: 19 October 2017 / Accepted: 6 March 2018 / Published online: 8 March 2018

Abstract Dissolution, dispersion, and aggregation characteristics of 2-hydroxy-3-trimethylammoniopropyl polysaccharides made from β-1,3-glucan extracted from *Euglena* (referred to as paramylon) differing in the degree of substitution (DS) of a 2-hydroxy-3-trimethylammoniopropyl group were examined. Freeze-dried solids made from cationic paramylon derivatives with a DS ranging from 0.07 to 0.16 spontaneously formed crystalline nanofibers upon being mechanically stirred in water. Derivatives with a DS greater than 0.31 lacked similar fiber formability. Nevertheless, they formed a distinctly outlined, transparent thin film featuring a nanometer-level flat surface using an aqueous solution casting method in which water is gradually removed from the aqueous homogeneous solution and a methanolic solution casting method featuring rapid removal of methanol from a heterogeneous solution. Those that had a DS less than 0.06 lacked solution solubility and dispersibility; they formed a thin film from a heterogeneous solution. These results demonstrate that cationic paramylon derivatives can be used as a constituent of well-organized polymeric materials.

Keywords β-1,3-Glucan · Paramylon · *Euglena* · Cationization · Nanofiber · Film

Introduction

The creation of materials from naturally occurring products has become an important research area. Specifically, the feasibility of using polysaccharides such as cellulose, chitin, and chitosan as a starting material has been intensively examined over the past decades (Edgar et al. 2001; Ifuku et al. 2013; Ifuku and Saimoto 2012; Isogai et al. 2011; Iwatake et al. 2008; Marubayashi et al. 2014; Puanglek et al. 2017; Teramoto et al. 2002). Our efforts in this area have focused on the use of algal β-1,3-glucan extracted from *Euglena* (referred to as paramylon) as a starting material for high-value-added products (Shibakami 2017; Shibakami and Sohma 2017; Shibakami et al. 2012, 2013a, b, 2014a, 2015). Paramylon is a storage

Electronic supplementary material The online version of this article (https://doi.org/10.1007/s10570-018-1740-4) contains supplementary material, which is available to authorized users.

M. Shibakami (✉) · T. Nemoto
Biomedical Research Institute, National Institute of Advanced Industrial Science and Technology (AIST), Central 6th, 1-1-1 Higashi, Tsukuba, Ibaraki 305-8566, Japan
e-mail: moto.shibakami@aist.go.jp

M. Sohma
Advanced Coating Technology Research Center, National Institute of Advanced Industrial Science and Technology (AIST), Central 5th, 1-1-1 Higashi, Tsukuba, Ibaraki 305-8565, Japan

polysaccharide stored as micrometer-sized spheroidal particles in large quantities inside the euglenoid cell (Barsanti et al. 2001; Santek et al. 2012). A structural feature of paramylon is that it adopts a helical conformation such as a triplex (Booy et al. 1981; Clarke and Stone 1960). This "helix formability" primarily prompted us to explore the feasibility of using paramylon as a biomass for materials with the expectation of it having functions differing from those of β-1,4-glucans such as cellulose, chitin, and chitosan.

Microscopic and X-ray diffraction observations revealed that the triplexes form a fibrous bundle and that the bundles hierarchically organize into spheroidal particles (Bluhm and Sarko 1977; Chuah et al. 1983; Deslandes et al. 1980; Marchessault and Deslandes 1979). This spontaneous aggregation characteristic is apparently an inherent structural property of paramylon, differentiating it from other glucans. This makes paramylon and its derivatives promising materials for developing high-value-added materials through oriented aggregation. Of particular importance for material creation is that the polysaccharides should have a dispersion characteristic other than oriented aggregation because such aggregation in the liquid phase requires that the polysaccharides be in a dispersed state prior to aggregation. A promising means of dispersion other than the use of a good solvent is chemical modification. Specifically, succinylation and carboxymethylation produce water-soluble paramylon derivatives, some of which form nanofibers in an aqueous environment (Shibakami 2017; Shibakami et al. 2013b, 2016). Thus, the introduction of anionic functional groups should be a useful means for providing paramylon with both dispersion and oriented aggregation characteristics.

The benefits of anionization prompted us to explore the feasibility of cationization. Although cationic 2-hydroxy-3-trimethylammoniopropyl paramylon has been synthesized as a potential antimicrobial agent (Sakagami et al. 1989), its dissolution, dispersion, and aggregation characteristics have received little or no attention. Our working assumption was threefold. First, creation of spontaneously occurring well-oriented aggregates made from cationic paramylon derivatives requires both water dispersibility due to using the cationic functional group and the oriented aggregability inherent to β-1,3-glucans. Second, the component polymer needs a suitable balance between these two conflicting characteristics. Third, the aggregation mode depends on the balance.

To specify the chemical structure of derivatives capable of forming well-oriented aggregates and to explore the dependence of the aggregation mode on the structure, a wide variety of cationic paramylon derivatives differing in the degree of substitution (DS) of the cationic functional group (DS_{hta}, average number of functional groups attached to a glucose unit) were synthesized. Their dissolution, dispersion, and aggregation characteristics were examined using dynamic light scattering, electrophoretic light scattering, visible spectroscopy, viscometry, microscopy, and X-ray diffractometry. Specifically, the cationic paramylon derivatives that had DS_{hta} ranging from 0.07 to 0.16 were found to spontaneously form nanofibers in water, indicating that this range is suitable for producing polysaccharides with well-balanced dispersibility and aggregability. The derivatives that had DS_{hta} outside this range failed to form any noticeable oriented aggregates in aqueous media. That is, those with DS_{hta} greater than 0.31 had little aggregability and high solubility in water while those with DS_{hta} less than 0.06 had little or no dispersibility in water. The formation of films from cationic paramylon derivatives with less dispersibility and/or aggregability was also investigated.

Experimental

General methods

^{1}H, ^{13}C, and ^{1}H–^{13}C-2D NMR [heteronuclear multiple quantum correlation (HMQC)] were recorded on a 500 MHz spectrometer (AVANCE 500, Bruker). 3-Trimethylsilyl propionic acid sodium salt-d_4 was used as an internal standard for the 2-hydroxy-3-trimethylammoniopropyl paramylons and the paramylon. Dimethyl sulfoxide (DMSO) was used as an internal standard for the acetylated 2-hydroxy-3-trimethylammoniopropyl paramylon, Quantitative ^{13}C NMR spectrum was obtained using the inverse-gated decoupling method. FT-IR spectra were recorded using a spectrophotometer (FT/IR-480ST, JASCO) equipped with an attenuated total reflectance accessory (ATR Pro 400-S, ZnSe prism, JASCO) with a resolution of 4 cm^{-1}. DS_{hta} was determined by comparing the integral values of the methyl protons of

the 2-hydroxy-3-trimethylammoniopropyl group with those of the glucose protons of the cationic paramylon derivatives in the ^{1}H NMR spectrum. All chemicals and reagents are commercially available and were used without further purification. The paramylon, which was extracted from *Euglena gracilis* Strain EOD-1 (Deposit Number FERM BP-11530), was donated by KOBELCO Eco-Solutions Co., Ltd. The ^{1}H and ^{13}C NMR spectra, FT-IR spectrum, weight average molecular weight (M_w), and number average molecular weight (M_n) of the paramylon were as follows: ^{1}H NMR (1.0 mol/L NaOD/D_2O, δ): 4.72 (m, 1H; H1), 3.93–3.45 (m, 6H; H2–H6). ^{13}C NMR (1.0 mol/L NaOD/D_2O, δ) 106.3 (C1), 89.9 (C3), 79.6 (C5), 76.6 (C2), 72.3 (C4), 64.1 (C6); FT-IR (cm^{-1}) 3361, 2899, 1118, 1078, 1040, 885; M_w 1.892 × 10^5; and M_n 1.531 × 10^5 (Shibakami 2017).

Synthesis of 2-hydroxy-3-trimethylammoniopropyl paramylon (products **1**–**8**)

To a homogeneous solution made from the paramylon (1.006 g, 6.205 mmol) and a 1.0-mol/L NaOH aqueous solution (50 mL) was added dropwise glycidyltrimethylammonium chloride (0.321 g of a 72.6-wt% aqueous solution, 1.536 mmol) at room temperature. The mixture was heated at ∼ 70 °C for 3.0 h and then allowed to cool to ambient temperature. After the solution was acidified to pH ∼ 1.0 by adding a concentrated hydrochloric acid aqueous solution, it was immediately poured into ethanol (100 mL) to precipitate a white solid. The resulting solid was separated by centrifugation. The solid was then dissolved in water (25 mL), followed by dialysis (regenerated cellulose, MWCO = 12,000–14,000, Fisher Scientific) against water overnight. Freeze-drying overnight resulted in product **1** (DS0.01), a cottony solid (575 mg, 2.869 mmol, yield 46.2%). Successful preparation was confirmed by ^{1}H and ^{13}C NMR and FT-IR measurements. ^{1}H NMR (1.0 mol/L NaOD/D_2O, δ): 4.73 (m, 1H; H1), 4.33 (m, 0.01H; H8), 3.94–3.47 (m, 6.04H; H2–H7, H9), 3.25–3.22 (m, 0.09H; H10). ^{13}C NMR (1.0 mol/L NaOD/D_2O, δ): 106.5 (C1), 90.0 (C3), 79.7 (C5), 76.7 (C2), 71.8 (C4), 64.2 (C6). FT-IR (cm^{-1}): 3296 (s), 2901 (m), 1652 (w), 1363 (w), 1107 (m), 1026 (s), 888 (m). DS_{hta} = 0.01.

A process similar to that described for the preparation of product **1** (DS0.01) except for using a feed molar ratio of 1:0.5 for the paramylon:glycidyltrimethylammonium chloride was used to obtain a 46.5% yield of product **2** (DS0.03) (592 mg, 2.925 mmol) from the paramylon (1.018 g, 6.279 mmol) and glycidyltrimethylammonium chloride (0.647 g of a 72.6-wt% aqueous solution, 3.098 mmol). Successful preparation was confirmed by ^{1}H and ^{13}C NMR and FT-IR measurements. ^{1}H NMR (1.0 mol/L NaOD/D_2O, δ): 4.73 (m, 1H; H1), 4.39–4.34 (m, 0.03H; H8), 3.94–3.41 (m, 6.12H; H2–H7, H9), 3.25–3.22 (m, 0.27H; H10). ^{13}C NMR (1.0 mol/L NaOD/D_2O, δ): 106.5 (C1), 90.0 (C3), 79.7 (C5), 76.7 (C2), 71.8 (C4), 64.2 (C6), (C10). FT-IR (cm^{-1}): 3296 (s), 2885 (m), 1155 (w), 1017 (s), 897 (m). DS_{hta} = 0.03.

A process similar to that described for the preparation of product **1** (DS0.01) except for using a feed molar ratio of 1:1 for the paramylon:glycidyltrimethylammonium chloride was used to obtain a 59.6% yield of product **3** (DS0.06) (762 mg, 3.699 mmol) from the paramylon (1.006 g, 6.205 mmol) and glycidyltrimethylammonium chloride (1.286 g of a 72.6-wt% aqueous solution, 6.157 mmol). Successful preparation was confirmed by ^{1}H and ^{13}C NMR and FT-IR measurements. ^{1}H NMR (1.0 mol/L NaOD/D_2O, δ): 4.73 (m, 1H; H1), 4.39–4.34 (m, 0.06H; H8), 3.94–3.47 (m, 6.24H; H2–H7, H9), 3.25–3.22 (m, 0.54H; H10). ^{13}C NMR (1.0 mol/L NaOD/D_2O, δ): 106.5 (C1), 90.0 (C3), 79.6 (C5), 76.7 (C2), 71.7 (C4), 64.2 (C6), 57.0 (C10). FT-IR (cm^{-1}): 3308 (s), 2909 (m), 1652 (w), 1363 (w), 1155 (m), 1030 (s), 886 (m). DS_{hta} = 0.06.

A process similar to that described for the preparation of product **1** (DS0.01) except for using a feed molar ratio of 1:1.5 for the paramylon:glycidyltrimethylammonium chloride was used to obtain a 55.6% yield of product **4** (DS0.07) (716 mg, 3.453 mmol) from the paramylon (1.006 g, 6.205 mmol) and glycidyltrimethylammonium chloride (1.928 g of a 72.6-wt% aqueous solution, 9.231 mmol). Successful preparation was confirmed by ^{1}H and ^{13}C NMR and FT-IR measurements. ^{1}H NMR (1.0 mol/L NaOD/D_2O, δ): 4.73 (m, 1H; H1), 4.39–4.34 (m, 0.07H; H8), 3.94–3.48 (m, 6.28H; H2–H7, H9), 3.25–3.22 (m, 0.63H; H10). ^{13}C NMR (1.0 mol/L NaOD/D_2O, δ): 106.5 (C1), 90.1 (C3), 79.8 (C5), 76.8 (C2), 71.8 (C4), 64.3 (C6), 56.9 (C10). FT-IR (cm^{-1}) 3292 (s), 2882 (m), 1363 (w), 1116 (m), 1026 (s), 885 (w). DS_{hta} = 0.07.

A process similar to that described for the preparation of product **1** (DS0.01) except for using a feed molar ratio of 1:2 for the paramylon:glycidyltrimethylammonium chloride was used to obtain a 42.4% yield of product **5** (DS0.11) (562 mg, 2.635 mmol) from the paramylon (1.009 g, 6.223 mmol) and glycidyltrimethylammonium chloride (2.565 g of a 72.6-wt% aqueous solution, 12.281 mmol). Successful preparation was confirmed by ^{1}H and ^{13}C NMR and FT-IR measurements. ^{1}H NMR (1.0 mol/L NaOD/D_2O, δ): 4.73 (m, 1H; H1), 4.38–4.31 (m, 0.11H; H8), 3.94–3.46 (m, 6.44H; H2–H7, H9), 3.25–3.21 (m, 0.99H; H10). ^{13}C NMR (1.0 mol/L NaOD/D_2O, δ): 106.5 (C1), 90.0 (C3), 79.7 (C5), 76.7 (C2), 71.8 (C4), 64.2 (C6), 56.9 (C10). FT-IR (cm^{-1}): 3327 (s), 2916 (m), 1645 (w), 1363 (w), 1119 (m), 1043 (s), 1037 (s), 887 (w). DS_{hta} = 0.11.

A process similar to that described for the preparation of product **1** (DS0.01) except for using a feed molar ratio of 1:3 for the paramylon:glycidyltrimethylammonium chloride was used to obtain a 57.3% yield of product **6** (DS0.16) (773 mg, 3.531 mmol) from the paramylon (1.000 g, 6.167 mmol) and glycidyltrimethylammonium chloride (3.866 g of a 72.6-wt% aqueous solution, 18.510 mmol). Successful preparation was confirmed by ^{1}H and ^{13}C NMR and FT-IR measurements. ^{1}H NMR (1.0 mol/L NaOD/D_2O, δ): 4.72 (m, 1H; H1), 4.36–4.30 (m, 0.16H; H8), 3.94–3.45 (m, 6.64H; H2–H7, H9), 3.25–3.21 (m, 1.44H; H10). ^{13}C NMR (1.0 mol/L NaOD/D_2O, δ): 106.5 (C1), 90.0 (C3), 79.7 (C5), 76.7 (C2), 73.8 (C7), 71.8 (C4), 68.0 (C9), 66.1 (C8), 64.2 (C6), 57.0 (C10). FT-IR (cm^{-1}) 3301 (s), 2881 (m), 1646 (m), 1363 (w), 1119 (w), 1030 (s), 888 (m). DS_{hta} = 0.16.

A process similar to that described for the preparation of product **1** (DS0.01) except for using a feed molar ratio of 1:7.5 for the paramylon:glycidyltrimethylammonium chloride was used to obtain a 84.1% yield of product **7** (DS0.31) (1.248 g, 5.195 mmol) from the paramylon (1.002 g, 6.180 mmol) and glycidyltrimethylammonium chloride (9.632 g of a 72.6-wt% aqueous solution, 46.117 mmol). Successful preparation was confirmed by ^{1}H and ^{13}C NMR and FT-IR measurements. ^{1}H NMR (1.0 mol/L NaOD/D_2O, δ): 4.74 (m, 1H; H1), 4.40–4.34 (m, 0.31H; H8), 3.94–3.49 (m, 7.24H; H2–H7, H9), 3.26–3.22 (m, 2.79H; H10). ^{13}C NMR (1.0 mol/L NaOD/D_2O, δ): 106.5 (C1), 90.0 (C3), 79.7 (C5), 76.8 (C2), 74.2 (C7), 71.8 (C4), 68.0 (C9), 68.0 (C8), 64.2 (C6), 57.0 (C10). FT-IR (cm^{-1}): 3322 (s), 2881 (m), 1635 (m), 1363 (w), 1121(m), 1032 (s), 910 (m). DS_{hta} = 0.31; M_w 2.728 × 10^5; M_n 2.014 × 10^5.

A process similar to that described for the preparation of product **1** (DS0.01) except for using a feed molar ratio of 1:15 for the paramylon:glycidyltrimethylammonium chloride was used to obtain a 54.4% yield of product **8** (DS0.64) (0.967 g, 3.342 mmol) from the paramylon (0.996 g, 6.143 mmol) and glycidyltrimethylammonium chloride (19.284 g of a 72.6-wt% aqueous solution, 92.331 mmol). Successful preparation was confirmed by ^{1}H and ^{13}C NMR and FT-IR measurements. ^{1}H NMR (1.0 mol/L NaOD/D_2O, δ): 4.73 (m, 1H; H1), 4.40–4.34 (m, 0.64H; H8), 3.94–3.47 (m, 8.56H; H2–H7, H9), 3.25–3.22 (m, 5.76H; H10). ^{13}C NMR (1.0 mol/L NaOD/D_2O, δ): 106.6 (C1), 90.1 (C3), 79.7 (C5), 77.5 (C2), 74.3 (C7), 71.7 (C4), 68.0 (C9), 64.2 (C6, C8), 56.9 (C10). FT-IR (cm^{-1}): 3301 (s), 2900 (m), 1473 (w), 1373 (w), 1127 (w), 1036 (s), 909 (m). DS_{hta} = 0.64; M_w 3.099 × 10^5; M_n 2.199 × 10^5.

Acetylation of 2-hydroxy-3-trimethylammoniopropyl paramylon (product **9**)

Product **8** (DS0.64) (366 mg, 1.504 mmol), acetic acid (14.4 mL), acetic anhydride (10.8 mL), and sulfuric acid (70 μL) were placed in a round-bottomed flask. The mixture was mechanically stirred for 21 h at ambient temperature under a nitrogen atmosphere. A white precipitate was separated from the resulting solution by decantation. The precipitate was washed with methanol (50 mL) by mechanical stirring for 30 min, followed by vacuum-drying for 1 h, yielding acetylated 2-hydroxy-3-trimethylammoniopropyl paramylon (product **9**) (39.4 mg, 0.115 mmol, yield 7.6%) as a white solid. Acetylation of product **8** (DS0.64) was confirmed by ^{1}H and ^{13}C NMR and FT-IR measurements. ^{1}H NMR (DMSO-d_6, δ): 4.75–3.32 (m, 9.2H; H1–H9), 3.21–3.52 (m, 5.8H; H10), 2.25–1.95 (m, 7.1H; CH_3CO). ^{13}C NMR (DMSO-d_6, δ): 171.0–169.2 (CH_3CO), 99.7 (C1), 78.4–61.7 (C2–C9), 53.4 (C10), 21.5–18.6 (CH_3CO). FT-IR (cm^{-1}): 1734 (s), 1372 (m), 1217 (s), 1029 (s), 913 (w).

Size exclusion chromatography with multiangle laser light scattering (SEC–MALLS) of 2-hydroxy-3-trimethylammoniopropyl paramylons

The M_w and M_n of products **7** (DS0.31) and **8** (DS0.64) were determined using SEC–MALLS measurements performed using a multiangle laser photometer (miniDAWN Treos, Wyatt Technology) and a refractive index detector (RI-501, Shodex) equipped with a gel permeation chromatography column (SB-806M HQ, Shodex) (50 mmol/L acetic acid in 0.2 mol/L $NaNO_3$ aqueous solution, 40 °C, 1.0 mL/min). The solutions were purified using a 0.20-μm filter. The injection volume was 100 μL with a concentration of 4.0 mg/mL. The *dn*/*dc* value was 0.1462.

Dynamic light scattering and electrophoretic light scattering of aqueous solutions containing 2-hydroxy-3-trimethylammoniopropyl paramylons

Homogeneous solutions with a concentration of 0.1-wt% were prepared from a freeze-dried solid of products **5** (DS0.11) and **7** (DS0.31) and a 10-mM NaCl aqueous solution using vortexing and sonicating. The resulting homogeneous solutions were subjected to dynamic light scattering and electrophoretic light scattering measurements with a zeta-potential & particle size analyzer (ELSZ-2000ZS, Otsuka Electronics). The measurements were conducted in triplicate at 25 °C.

Light transmittance spectroscopy of aqueous solutions containing 2-hydroxy-3-trimethylammoniopropyl paramylons

A mixture made from a freeze-dried solid of the cationic paramylon derivative (100 mg) and Milli-Q water (10 mL) was mechanically stirred for 20 h. The resulting homogeneous solution containing products **4** (DS0.07)–**8** (DS0.64) was then transferred in a cuvette (10-mm path length) to evaluate visible light transmission. The light transmittance spectrum was measured using a spectrophotometer (UV-2500, Shimadzu).

Viscometry of aqueous solutions containing 2-hydroxy-3-trimethylammoniopropyl paramylons

A mixture made from a freeze-dried solid of the cationic paramylon derivative (100 mg) and Milli-Q water (10 mL) was mechanically stirred for 1 h. The viscosity of the homogeneous solution containing products **4** (DS0.07)–**8** (DS0.64) was then measured with a viscometer (DV1M, EKO Instruments) using three types of spindles (SC4-14, SC4-21, and SC4-34, EKO Instruments) at various rotation rates (0.3–100 rpm) at 23 °C.

Preparation of thin films from 2-hydroxy-3-trimethylammoniopropyl paramylons

A solution made from a freeze-dried solid of the cationic paramylon derivative (30 mg) and Milli-Q water (2.0 mL) or methanol (2.0 mL) was placed in a polytetrafluoroethylene dish with a diameter of 25 mm. After removal of the solvent, a thin film formed in the dish. Light transmittance spectroscopy was performed using a spectrophotometer (UV-2500, Shimadzu) on solution-cast films made from products **7** (DS0.31) and **8** (DS0.64).

Scanning electron microscopy (SEM) of freeze-dried solids made from 2-hydroxy-3-trimethylammoniopropyl paramylons

A freeze-dried solid of the cationic paramylon derivative (10 mg) was placed in a flask containing Milli-Q water (10 mL). The solution was mechanically stirred for ~ 20 h. It was then quickly frozen with liquid nitrogen followed by drying under reduced pressure, resulting in a cottony solid. This solid was fixed on a microscope metal stage using carbon conductive double-sided tape. SEM observations were carried out under high vacuum using a 5- or 10-kV accelerating voltage and a scanning electron microscope (JSM-6060, JEOL).

Wide-angle X-ray diffractometry (WAXD) of freeze-dried and air-dried solids made from 2-hydroxy-3-trimethylammoniopropyl paramylons

WAXD measurements were performed on freeze-dried and air-dried solids of products **4** (DS0.07), **5**

(DS0.11), and **6** (DS0.16) using an X-ray diffractometer (RINT 2550 V, Rigaku) with monochromatic Cu-Kα radiation (λ = 0.15418 nm) generated at 40 kV and 200 mA through an optical slit system: divergence slit = 0.5°; scattering slit = 0.5°; and receiving slit = 0.3 mm. Scattering was performed for a scattering angle 2θ of 2°–60° with a 2θ step of 0.05° and a scan speed of 5°/min.

Scanning probe microscopy (SPM) of evaporation residues and thin films made from 2-hydroxy-3-trimethylammoniopropyl paramylons

SPM observations were carried out using a scanning probe microscope (SPI4000/SPA-400, SII) containing a 20-mm scanner in tapping mode. One drop (5 µL) of aqueous solution containing products **4** (DS0.07)–**6** (DS0.16) (0.1 mg/mL) was placed on a freshly cleaved mica surface. After removal of residual water in the air, the resulting residue was observed using a microcantilever (SI-DF40, SII) at ambient temperature. The surfaces of polysaccharide films made from product **7** (DS0.31) fixed on a microscope metal stage using double-sided tape were observed using a similar method.

Results and discussion

Synthesis of 2-hydroxy-3-trimethylammoniopropyl paramylons

The reactions for preparing the 2-hydroxy-3-trimethylammoniopropyl paramylons (**1**–**8**) using a feed molar ratio of 1:0.25 to 1:15 for paramylon:glycidyltrimethylammonium chloride are shown in Scheme 1. Figure 1a shows the FT-IR spectra of product **6** (DS0.16) and the paramylon. The strong absorption around 3300 cm^{-1} was due to the hydroxyl groups of the paramylon and the 2-hydroxy-3-trimethylammoniopropyl group.

Fig. 1 **a** FT-IR spectra of 2-hydroxy-3-trimethylammoniopropyl paramylon [product **6** (DS0.16)] and paramylon, **b** ^{1}H NMR spectrum, **c** ^{13}C NMR spectrum; inset shows magnification of ^{13}C NMR spectrum (∼ 60 to ∼ 74 ppm), **d** ^{1}H–^{13}C-2D (HMQC) NMR spectrum of product **6** (DS0.16), **e** ^{1}H–^{13}C-2D (HMQC) NMR spectrum of paramylon, **f** FT-IR spectrum, and **g** quantitative ^{13}C NMR spectrum of acetylated 2-hydroxy-3-trimethylammoniopropyl paramylon [product **8** (DS0.64)] (product **9**); inset shows magnification and deconvolution of ^{13}C NMR (∼ 169 to ∼ 171 ppm) of product **9**

Figure 1b–e shows the ^{1}H, ^{13}C, and ^{1}H–^{13}C-2D (HMQC) NMR spectra of product **6** (DS0.16) and the paramylon, respectively. The 1D NMR signal assignments were made using the spectra of 2-hydroxy-3-trimethylammoniopropyl polysaccharides made from curdlan and dextran, structural analogs of the present products (Nichifor et al. 2010; Suflet et al. 2015) and the 2D NMR spectra of product **6** (DS0.16) and the paramylon.

The glucose protons and carbons of product **6** (DS0.16) showed virtually the same spectra as those of the paramylon. In brief, the ^{1}H NMR signal appeared around 4.7 ppm and the ^{13}C NMR signal at 106.5 ppm were assigned to H1 and C1, respectively based on the appearance of a clear cross peak in the 2D NMR spectra. This ^{1}H resonance of the product **6** (DS0.16) was split into two peaks. This split indicated that there are two different H1 protons in terms of magnetic field environment. The ^{13}C NMR signal appeared at 90.0 ppm, which is ascribed to C3, had a correlation signal around ∼ 3.7 ppm (H3). The ^{13}C signal appeared at 79.7 ppm, which is due to C5, had a weak cross peak at ∼ 3.5 ppm (H5). The ^{13}C NMR signal at 71.8 ppm, which is ascribable to C4, had a cross peak at ∼ 3.5 ppm (H4). The ^{13}C signal at 64.2 ppm, which is ascribable to C6, had two correlation signals at ∼ 3.9 and ∼ 3.7 ppm (H6, H6′). The signal due to

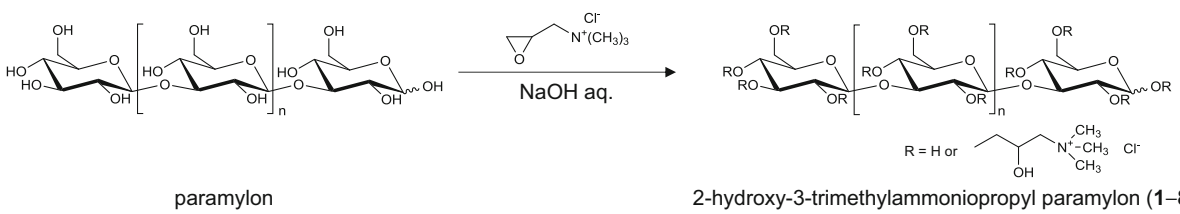

Scheme 1 Reactions used to prepare 2-hydroxy-3-trimethylammoniopropyl paramylons (**1**–**8**)

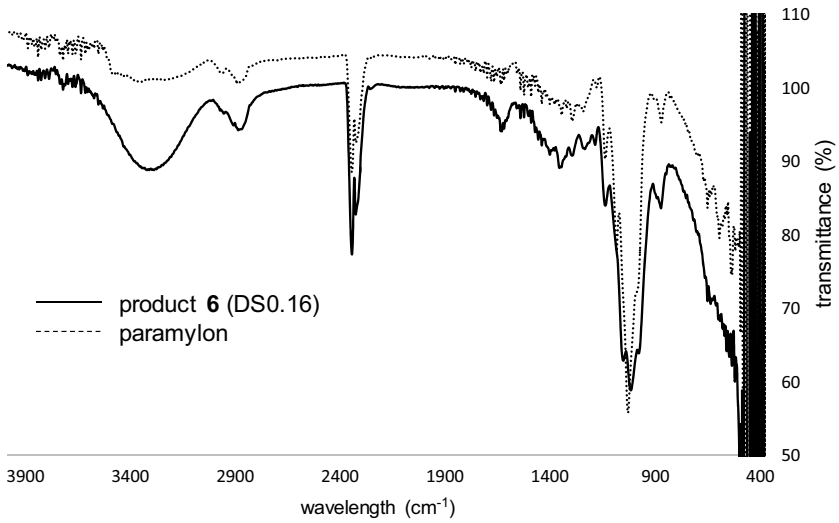
product 6 (DS0.16)
paramylon
transmittance (%)
wavelength (cm-1)

(a)

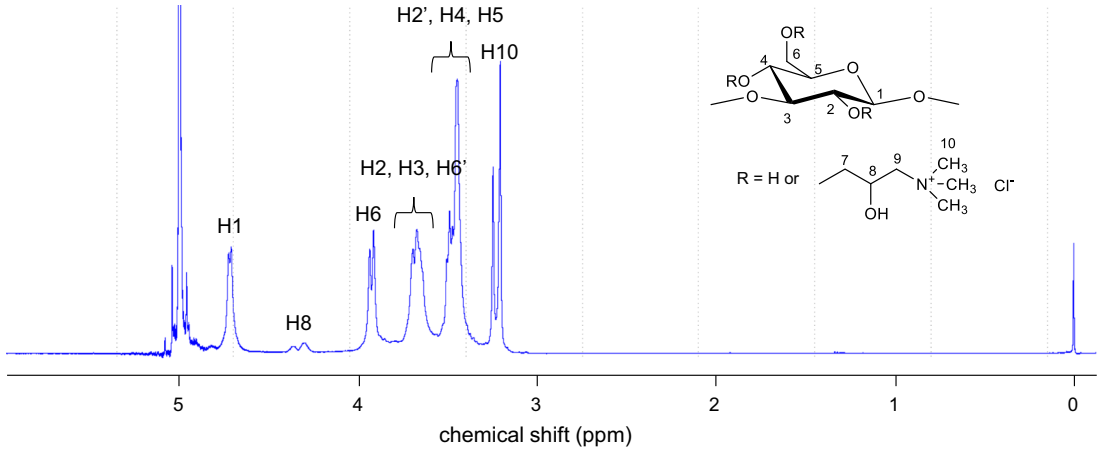
H2', H4, H5
H10
H2, H3, H6'
H6
H1
H8
R = H or
Cl-
chemical shift (ppm)

(b)

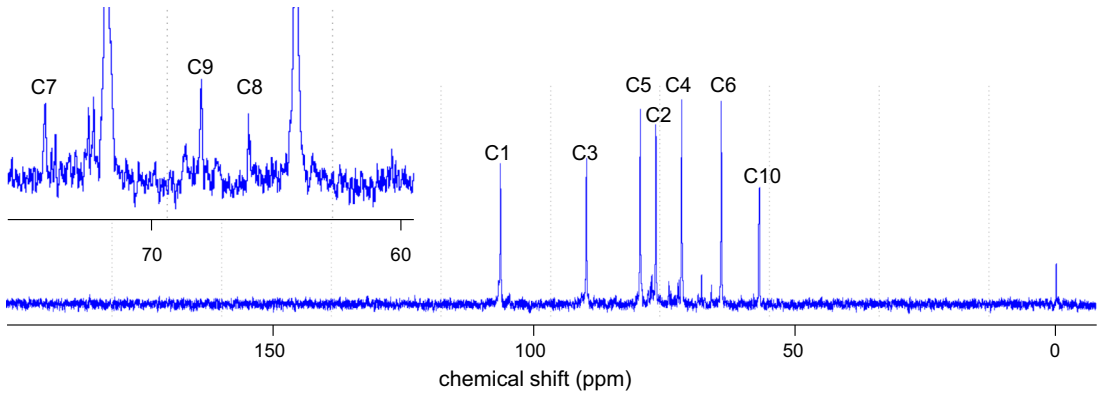
C7
C9
C8
C5
C4
C6
C2
C1
C3
C10
chemical shift (ppm)

(c)

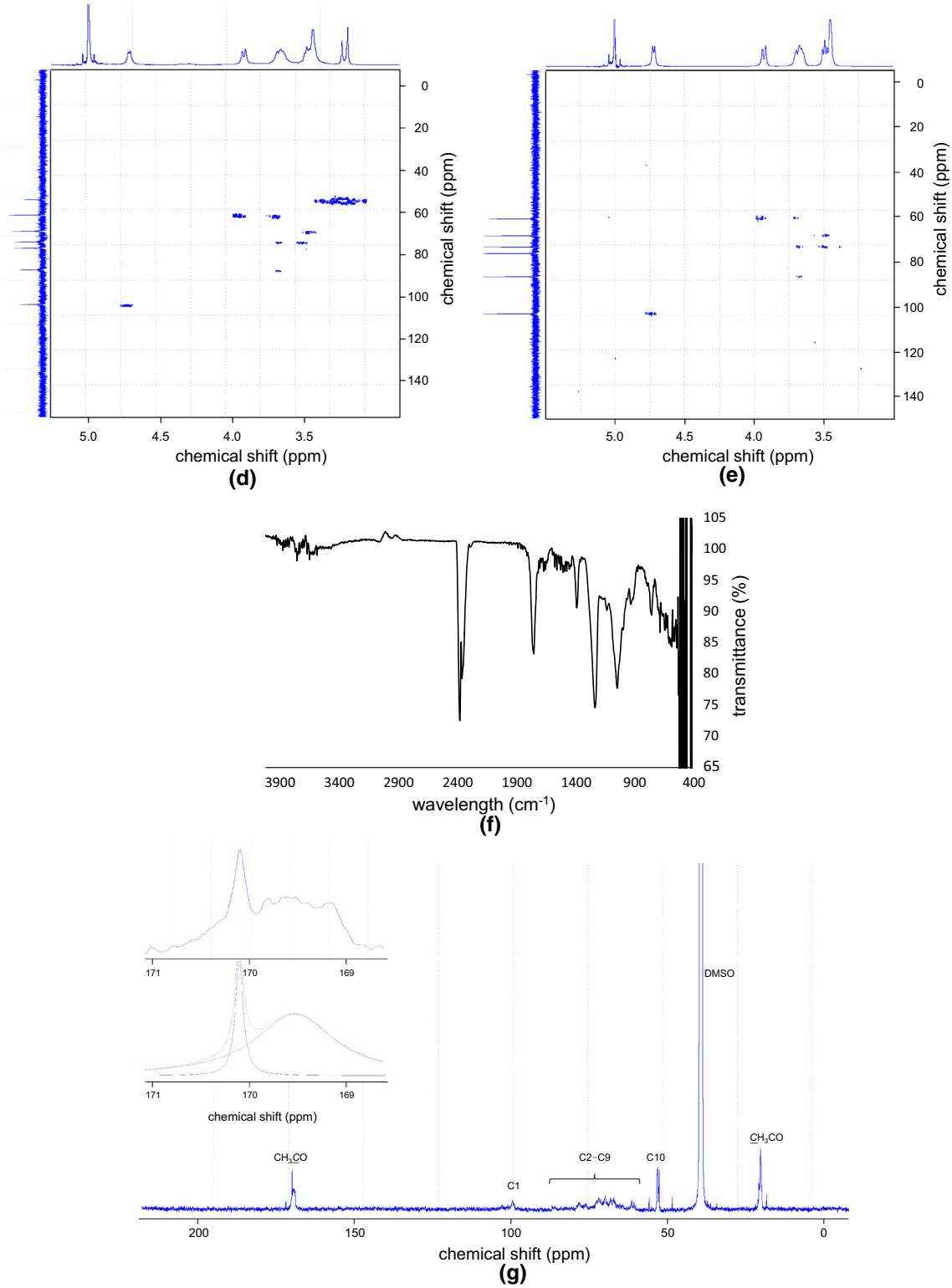

Fig. 1 continued

H6 was split into two, which is similar to the H1 signal. The ^{13}C signal at 76.7 ppm, which is due to C2, also had two correlation signals at ~ 3.7 and ~ 3.5 ppm (H2, H2′). The appearance of two correlation signals for one ^{13}C signal indicated that each carbon has two types of protons differing in magnetic field environment.

A strong cross peak observed at ~ 3.2 ppm (^{1}H signal) and ~ 57 ppm (^{13}C signal) is due to the methyl group (H10, C10) of the substituent. This ^{1}H resonance was split into two, indicating that two different H10 protons exist. A plausible reason for the split is that the substituent was not exclusively introduced into one hydroxyl group but into multiple ones.

No apparent cross peaks due to the substituent protons and carbons were observed in the 2D NMR. The 2D NMR spectrum of product **8** (DS0.64) also did not show any cross peaks due to H7–C7, H8–C8, and H9–C9 (supplementary data). The signal disappearance is likely attributable to the low DS_{hta} value of product **6** (DS0.16) as well as the decreased molecular mobility of the substituent associated with the increase in solution viscosity. Thus, the temporal signal assignments were made using the NMR spectra of the 2-hydroxy-3-trimethylammoniopropyl curdlan and the 2-hydroxy-*N*-dimethyl-*N*,*N*-butylammoniopropyl dextran (Nichifor et al. 2010; Suflet et al. 2015). Briefly, the ^{1}H signal appeared around 4.3 ppm is assigned to H8. The methylene protons (H7, H9) likely overlapped with the glucose protons (H2–H6). Further microstructural characterization of glucose and substituent protons remains to be elucidated because of the signal overlap. The faint ^{13}C NMR signals appeared at 73.8, 68.0, and 66.1 ppm were temporarily assigned to C7, C9, and C8, respectively. These NMR spectra indicate the successful introduction of the cationic functional group into the paramylon. The spectra of products **1** (DS0.01)–**7** (DS0.11→0.31) were similar except for the intensities of the signals due to the methyl groups of the substituent. DS_{hta} ranged from 0.01 to 0.64 (Table 1).

The paramylon has three different hydroxyl groups (at C2, C4, and C6) in a glucose unit. To determine the partial DS_{hta} for each hydroxyl group, a quantitative ^{13}C NMR measurement was performed on product **9** prepared by acetylating product **8** (DS0.64) (Tezuka 1993; Tezuka et al. 1991; Tezuka and Tsuchiya 1995). The strong absorption at 1733 cm^{-1} in the FT-IR spectrum and the signals around 170 and 20 ppm were due to the acetyl group (Fig. 1f, g). The intensities of the ^{13}C signals due to the glucose carbons (C1–C6) were low and broadened because the polymer motion was rather inhibited in the DMSO-d_6 solvent. The signals due to the methylene and methine carbons of the substituent (C7–C9) likely overlapped those of the glucose carbons. The signals, which is ascribable to the methyl carbons (C10), appeared at ~ 53 ppm.

Table 1 Degree of substitution (DS_{hta}), molecular weights (M_w, M_n), and degree of polymerization (DP) of 2-hydroxy-3-trimethylammoniopropyl paramylons and paramylon

Product	DS_{hta}	M_w (× 10^5)	M_n (× 10^5)	DP
1	0.01	–	–	–
2	0.03	–	–	–
3	0.06	–	–	–
4	0.07	–	–	–
5	0.11	–	–	–
6	0.16	–	–	–
7	0.31	3.099	2.199	1260
8	0.64	2.728	2.014	1332
Paramylon	0	1.892	1.531	1167

A close examination of the ^{13}C signal appeared at ~ 170 ppm revealed that it consists of a sharp signal at 170.1 ppm and a broad one around 169.6 ppm, and these signals overlapped. The former and the latter are ascribable to C-6 and C-2/C-4, respectively (Shibakami et al. 2014b). While it is likely that cationization barely occurred at C-4 given the higher steric hindrance at C-4 than at C-6 and C-2 and the bulkiness of the glycidyltrimethylammonium chloride, the signal was not assigned to C-2 and C-4 because of the proximity of the signals due to C-2 and C-4. The overlapping signals were deconvoluted using Bruker Topspin ver. 3.0 software, revealing that the integral ratios of the acetyl group obtained through deconvolution were 0.16 and 0.84 for C-6 and C-2/C-4, respectively. Given the DS_{hta} of product **8** (DS0.64) is 0.64, the partial DS_{hta} values for C-6 and C-2/C-4 are estimated to be 0.54 and 0.10, respectively. These values show that the cationization preferentially proceeds at the primary hydroxyl group.

Since paramylon is completely soluble in a 1.0-mol/L NaOH aqueous solution, it is evident that the introduction of the 2-hydroxy-3-

trimethylammoniopropyl group did not succeed for crystalline paramylon nanofibers fibrillated from the paramylon particles but did succeed for randomly coiled paramylon polymers. It is thus apparent that the cationic substituent groups were homogeneously introduced into the polymer. The aggregation of the cationic paramylon derivatives is discussed below on the basis of the WAXD results.

A question that needed to be answered prior to investigating dissolution, dispersion and aggregation was whether or not the degree of polymerization (DP) of the cationic paramylon derivatives maintains the original value of the paramylon after the cationization reaction has completed. To answer this question, SEC–MALLS was performed. Since only products **7** (DS0.31) and **8** (DS0.64) showed apparent high solubility in the mobile phase by naked eye observation, molecular weight determination by SEC–MALLS was performed on those two products; SEC–MALLS could not be performed on the other products because of their low or no solubility in the mobile phase and/or too high solution viscosity for filtration. Table 1 shows the molecular weights and DP of products **7** (DS0.31) and **8** (DS0.64), with the paramylon as a reference. The M_w and M_n of products **7** (DS0.31) and **8** (DS0.64) were $\sim$ 3.0 and $\sim$ 2.0×10^5, respectively. Both products had a DP of $\sim$ 1300, comparable to that of the paramylon. Although it is possible that a small aggregate was made from products **7** (DS0.31) and **8** (DS0.64) with molecular weights comparable to those of paramylon, it is likely that these polysaccharides did not suffer significant depolymerization under the present reaction conditions. If that is the case, significant depolymerization likely did not occur in the other products as well since all the products were synthesized under similar conditions.

Table 2 shows the radii and zeta potential values of the particles made from products **5** (DS0.11) and **7** (DS0.31), representative products in terms of low and high DS_{hta}, respectively, in an aqueous environment. It is evident that the larger the DS_{hta}, the higher the average radius. This result can be accounted for by the electrostatic repulsion between the positively charged 2-hydroxy-3-trimethylammoniopropyl groups. Further examination of the dynamic light scattering results indicates that the particles (excluding insoluble matter) roughly fall into two categories on the basis of the radius; a product **5** (DS0.11) solution contained 20.0–25.8- and 247.3–281.7-nm particles and a product **7** (DS0.31) one contained 23.9–26.4- and 418.8–598.6-nm particles. Thus, it is plausible that both single-strand- and/or triplex-based smaller particles and larger particles composed of smaller ones were dispersed in the 10-mM NaCl aqueous solution.

Table 2 Average radius and zeta potential of 2-hydroxy-3-trimethylammoniopropyl paramylons in 10-mM NaCl aqueous solution

Product	Average radius (nm)	Zeta potential (mV)
5	314.0 ± 33.2	12.19 ± 1.05
7	899.3 ± 59.4	23.40 ± 0.64

It is also evident that the larger the DS_{hta}, the higher the zeta potential, apparently because the number of cationic substituents for product **7** (DS0.31) was larger than that for product **5** (DS0.11).

Dissolution and dispersion characteristics in aqueous solution

Light transmittance spectroscopy of aqueous solutions containing 2-hydroxy-3-trimethylammoniopropyl paramylons

A working assumption was that the creation of well-oriented aggregates requires the component polysaccharides to have both water dispersibility due to using the cationic functional group and the oriented aggregability inherent to β-1,3-glucans in the aqueous solution as well as a suitable balance between these conflicting characteristics. To examine the dependence of the dispersibility on DS_{hta}, the transmittance spectra of 1.0-wt% homogeneous aqueous solutions containing the cationic paramylon derivatives were measured. Products **1** (DS0.01)–**3** (DS0.06) were not subjected to spectroscopy because their freeze-dried solids settled to the bottom of the sample bottle without being fully dissolved even after 20-h mechanical stirring.

As shown in Fig. 2, the transmittance of products **4** (DS0.07) and **6** (DS0.16) was more than 85%, and that of product **5** (DS0.11) was more than 75%, indicating that they had moderate dispersibility. The aqueous solutions of products **7** (DS0.31) and **8** (DS0.64) showed much higher transmittance (> 95%), which

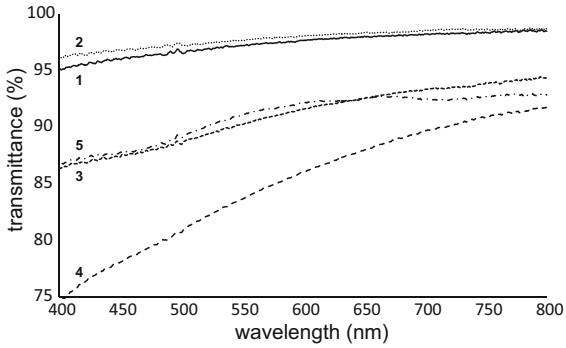

Fig. 2 Light transmittance spectra of aqueous solutions containing 2-hydroxy-3-trimethylammoniopropyl paramylons [**4** (DS0.07), **5** (DS0.11), **6** (DS0.16), **7** (DS0.31), and **8** (DS0.64)]

was due to electrostatic repulsion between the positively charged functional groups. Thus, the boundary DS_{hta} between high solubility and moderate dispersibility estimated by light transmittance spectroscopy was ∼ 0.16. An incidental finding was that only the aqueous solutions containing products **4** (DS0.07)–**6** (DS0.16) turned into a gel after standing overnight (Fig. 3). Specifically, the solutions containing products **4** (DS0.07) and **5** (DS0.11) were so viscous that a stirrer bar embedded in the solution did not fall out even when the sample bottle was turned upside down. The gel formation is assumed to have proceeded as follows. After the freeze-dried solids were dispersed in water, nanofibers gradually formed in the homogeneous aqueous solution when it was left standing overnight. Physical cross-linking of the nanofibers led to gel formation.

Viscometry of aqueous solutions containing 2-hydroxy-3-trimethylammoniopropyl paramylons

To further examine the dependence of solubility and dispersibility on DS_{hta}, freshly prepared homogeneous solutions containing products **4** (DS0.07)–**8** (DS0.64) were subjected to viscometry. The results are shown in Fig. 4. The significant difference in viscosity between products **5** (DS0.11) and **6** (DS0.16) and the small one between products **6** (DS0.16) and **7** (DS0.31) indicate that the boundary DS_{hta} between high solubility and moderate dispersibility was ∼ 0.16, comparable to that estimated by light transmittance spectroscopy.

Aggregation characteristic in aqueous solution

SEM observation of freeze-dried solids made from 2-hydroxy-3-trimethylammoniopropyl paramylons

As described above, the boundary DS_{hta} between high solubility and moderate dispersibility estimated by light transmittance spectroscopy and viscometry was ∼ 0.16. Since aggregability is inextricably associated with dispersibility, it is likely that the boundary DS_{hta} for aggregability also lies around 0.16. With this idea in mind, we used a SEM to observe freeze-dried solids made from the aqueous solutions to clarify the aggregation characteristic in aqueous media.

As shown in Fig. 5, most of the solids made from products **1** (DS0.01) and **2** (DS0.03) were amorphous or sheet-like structures. The freeze-dried solid of product **3** (DS0.06) contained fibers and amorphous structures. The solids made from products **4** (DS0.07)–**6** (DS0.16) were mainly composed of fibers with a diameter of ∼ 100 nm or less, and their fiber composition ratios were higher than that of the solid of

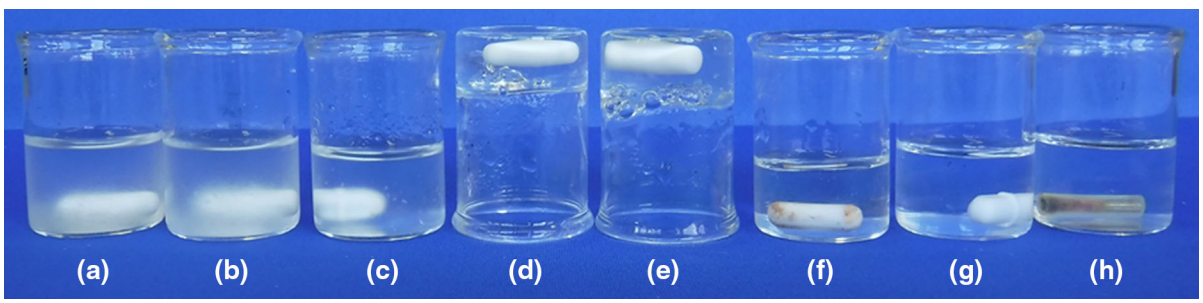

Fig. 3 Photographs of aqueous solutions containing 2-hydroxy-3-trimethylammoniopropyl paramylons after 20-h stirring followed by overnight standing: **a 1** (DS0.01), **b 2** (DS0.03), **c 3** (DS0.06), **d 4** (DS0.07), **e 5** (DS0.11), **f 6** (DS0.16), **g 7** (DS0.31), and **h 8** (DS0.64)

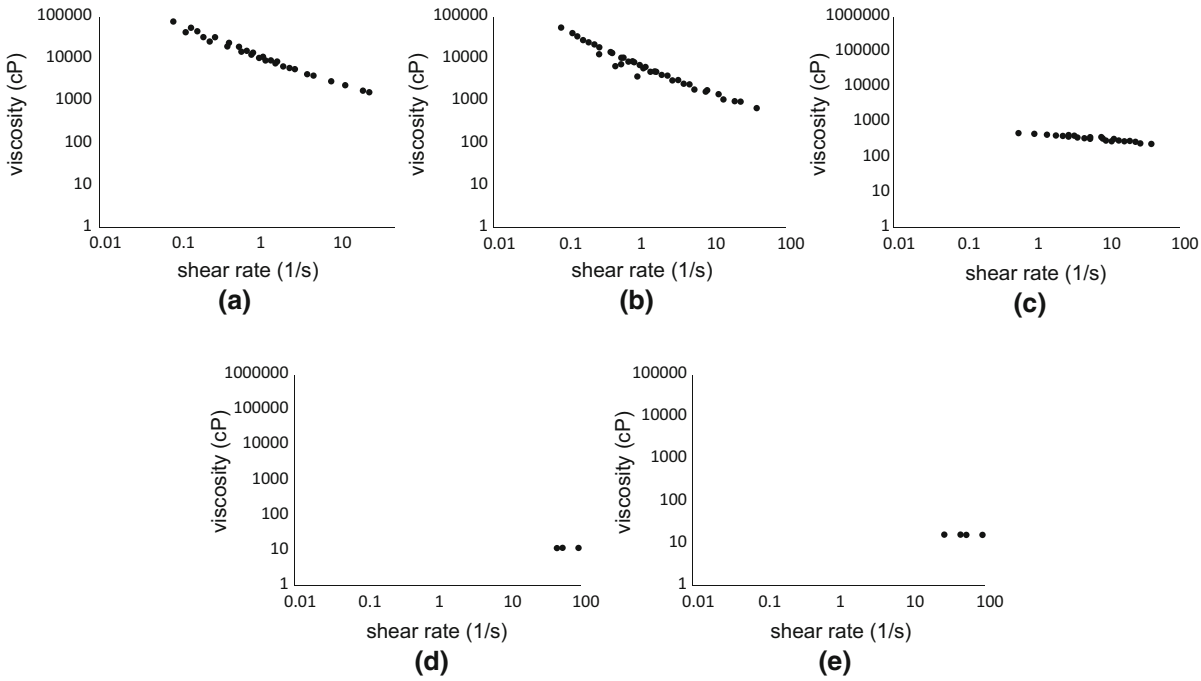

Fig. 4 Viscosity–shear rate relationship of aqueous solutions containing 2-hydroxy-3-trimethylammoniopropyl paramylons: **a 4** (DS0.07), **b 5** (DS0.11), **c 6** (DS0.16), **d 7** (DS0.31), and **e 8** (DS0.64)

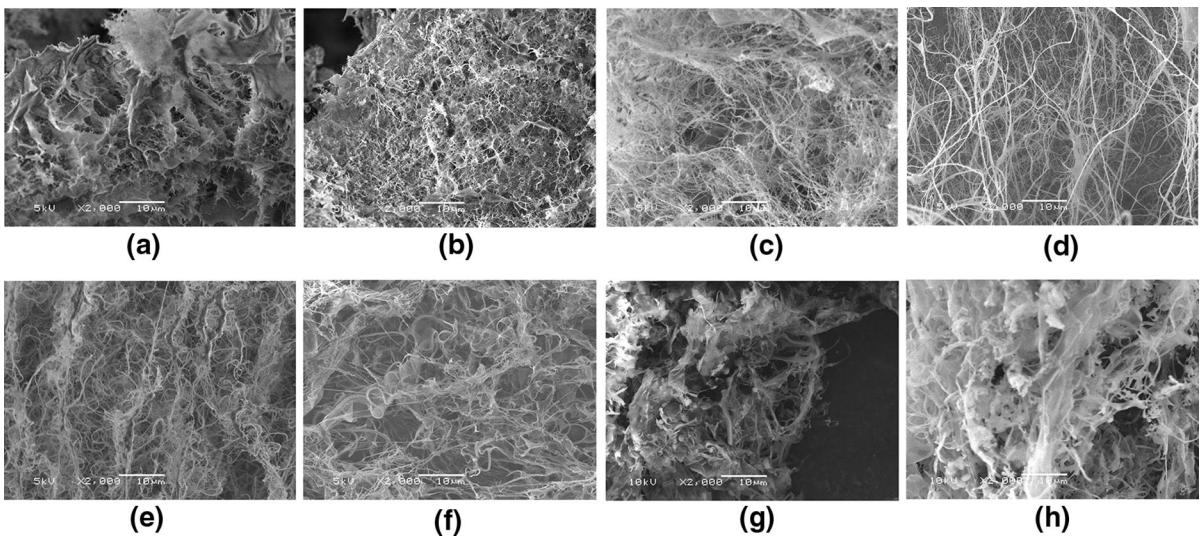

Fig. 5 Scanning electron microscopic images of freeze-dried solids made from 2-hydroxy-3-trimethylammoniopropyl paramylons: **a 1** (DS0.01), **b 2** (DS0.03), **c 3** (DS0.06), **d 4** (DS0.07), **e 5** (DS0.11), **f 6** (DS0.16), **g 7** (DS0.31), and **h 8** (DS0.64). Scale bar represents 10 μm

product **3** (DS0.06). Although the exact fiber length remains unclear, there were fibers several tens of micrometers or more long. Given that the diameter and length of a paramylon triplex estimated by X-ray crystallography are ∼ 1.6 and ∼ 365 nm (for a DP of 1167), respectively (Chuah et al. 1983), the observed fiber sizes are too large. A plausible explanation is that many single-strand polymers organized

in both the width and length directions, forming large fibrous structures in the aqueous environment. An alternative explanation that the fibers formed through water sublimation is unlikely because water sublimation rarely yields well-ordered structures such as fibers but rather amorphous or sheet-like aggregates, as frequently observed in the freeze-dried solids of products **1** (DS0.01), **2** (DS0.03), **7** (DS0.31), and **8** (DS0.64). Additional evidence for the fiber formation of products **4** (DS0.07)–**6** (DS0.16) was provided by SPM. The details are described below. Taken together, these results indicate that products **4** (DS0.07)–**6** (DS0.16) exhibited distinct oriented aggregation characteristics in the aqueous media by which they formed fibrous aggregates equal or similar in shape and size to those observed in the SEM images. Comparison of the SEM images revealed that the upper boundary DS_{hta} for fiber formation was ∼ 0.16, comparable to the boundary between high solubility and moderate dispersibility.

Wide angle X-ray diffraction measurements of freeze-dried solids made from 2-hydroxy-3-trimethylammoniopropyl paramylons

Given the low DS_{hta} values of products **4** (DS0.07)–**6** (DS0.16), it is possible that they formed crystalline nanofibers. To examine this idea, we performed WAXD measurements on the freeze-dried solids made from these products. As shown in Fig. 6, all the solids displayed a broad peak in the region of 2θ between ∼ 15 and ∼ 25° and a relatively sharper one around 6.3°. Product **4** (DS0.07) displayed an additional small peak around 12°. These results indicate that the nanofibers had a crystalline nature. Given that the paramylon showed a sharp diffraction peak at 6.4° (Kobayashi et al. 2010; Shibakami et al. 2012), the peak around 6.3° indicates that the nanofibers may have had a crystal structure close to that of the native paramylon. While further studies are required, this idea is plausible if we consider that a small amount of the cationic substituent was preferentially introduced into the hydroxyl group at C-6, as suggested by the quantitative ^{13}C NMR results and that the hydroxyl groups at C-2 and C-4 contribute to the formation of a helical crystal structure (Chuah et al. 1983).

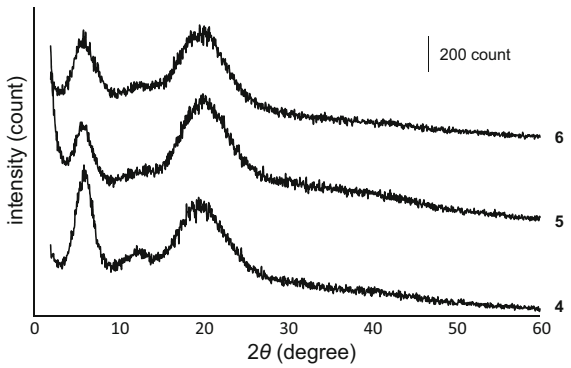

Fig. 6 Wide angle X-ray diffractograms of freeze-dried solids of products **4** (DS0.07), **5** (DS0.11), and **6** (DS0.16)

SPM observation of evaporation residues made from 2-hydroxy-3-trimethylammoniopropyl paramylons on mica

As described above, SEM revealed that products **4** (DS0.07)–**6** (DS0.16) had distinct nanofiber formation ability in water. To explore this oriented aggregability, SPM was performed on the evaporation residues of these products deposited on a mica surface. The working assumption was that, if nanofibers formed only through water sublimation, no fibers would be observed on the mica surface.

Figure 7 shows SPM images of the surface and cross-sections of the evaporation residues of products **4** (DS0.07)–**6** (DS0.16). The surface images show that fibrous structures with a length of less than 1 nm formed on the substrate. Since it is unlikely that water evaporation forms well-defined fibrous structures on a mica surface, this observation indicates that the fibers were not formed by water sublimation but were already present in the aqueous solution. The cross-sectional images show that their widths ranged from ∼ 50 to ∼ 80 nm and their heights from ∼ 1.8 to ∼ 4.6 nm. The fiber dimensions estimated from the SPM images are smaller than those observed in the SEM ones. The number of fibers in the SPM images was smaller than that in the SEM ones. We think that the differences in size and number are attributed to the difference in the water removal procedure in the sample preparation process as well as the ten times lower concentration of the SPM sample than the SEM one. That is, water was removed from the frozen sample for the SEM observations, which maintained the oriented aggregation mode already present in the aqueous media. The water was removed at ambient temperature under ordinary pressure for the

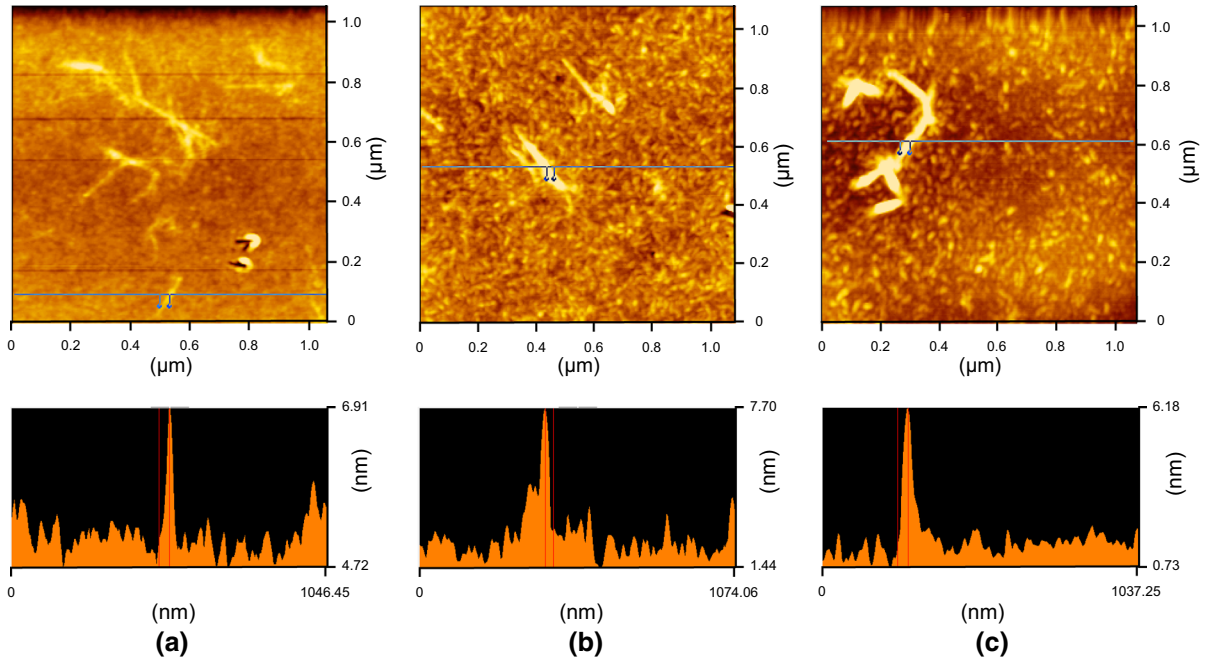

Fig. 7 Scanning probe microscopic images of surface and cross-section of nanofibers made from 2-hydroxy-3-trimethylammoniopropyl paramylons: **a 4** (DS0.07), **b 5** (DS0.11), and **c 6** (DS0.16)

SPM observation, which may have caused the ordered aggregates to collapse into air-stable nanometer-order crystalline structural elements if the fibrous aggregate structures were not strong enough to remain standing in atmosphere. This idea is plausible because the WAXD profiles showed that the films made from products **4** (DS0.07)–**6** (DS0.16) prepared by removing water at ambient temperature under ordinary pressure (i.e., aqueous solution casting described below) had a crystalline nature (Fig. 8). The interaction between the mica surface and the fibers in air may have contributed to the collapse of fibers.

Given the structural maintenance capability of the freeze-drying process, comparison between the SEM and SPM observation results indicates that the formation and maintenance of the fibrous structures made from products **4** (DS0.07)–**6** (DS0.16) require an aqueous environment. The fibrous structures observed in the SPM images were likely nanofibers that survived the water removal process.

Hypothesized nanofiber formation mechanism

While further studies for exploring the nanofiber formation mechanism are required, a plausible

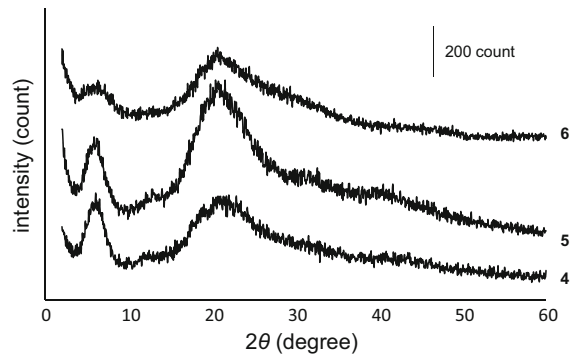

Fig. 8 Wide angle X-ray diffractograms of films of products **4** (DS0.07), **5** (DS0.11), and **6** (DS0.16)

mechanism based on the present results is as follows. The freeze-dried product solids of products **4** (DS0.07)–**6** (DS0.16) can be dispersed into nanometer-order crystalline structural elements less than visible-light wavelength in size upon the solid being poured in water. The structural elements then hierarchically reorganize into a fibrous structure in the aqueous media. This hierarchical fiber formation process and the maintenance of the fiber structure require an aqueous environment.

Aggregation characteristic in solution casting process

Preparation of films from 2-hydroxy-3-trimethylammoniopropyl paramylons

The primary purpose of introducing a 2-hydroxy-3-trimethylammoniopropyl group was to provide paramylon with both the dispersibility and oriented aggregability needed for developing polymeric materials. The successful fiber formation from products **4** (DS0.07)–**6** (DS0.16) likely stems from a suitable balance between the dispersion and aggregation characteristics. If that is the case, the unsuccessful formation of well-defined aggregates from products **7** (DS0.31) and **8** (DS0.64) in water can be attributed to the imbalance between these two conflicting characteristics due to their high water solubility for creating polymeric materials. An alternative means for inducing aggregation is forcible removal of water molecules from the neighborhood of the polymers.

A preparation method consistent with this idea is the solution casting method. There are two possible methods. One is the aqueous solution casting method in which water is gradually removed from the aqueous solution. We applied this method to all products. As shown in Fig. 9a–c, products **1** (DS0.01)–**3** (DS0.06) formed a slightly opaque, slightly convoluted thin film from a heterogeneous solution. This occurred because structural heterogeneity occurs when the size of the aggregate is larger than the wavelength of visible light during film preparation. Products **4** (DS0.07)–**6** (DS0.16) formed a convoluted or fragmented film from a viscous solution (Fig. 9d–f). The convoluted shape is attributed primarily to the viscous state of their aqueous solutions. The opaqueness is attributable to the convoluted shape and the structural heterogeneity induced by the larger aggregate formation with the removal of water. Unlike these films, a distinctly outlined, almost flat transparent thin film formed from products **7** (DS0.31) and **8** (DS0.64) from a homogeneous solution (Fig. 9g, h). The main driving force for this film preparation likely stems from the high water solubility of these products: the freeze-dried product solids disassembled into single-strand- and/or triplex-based structural elements smaller than the visible light wavelength upon the solids being soaked in water. This structural element may correspond to a particle with a diameter of $\sim$ 20 nm observed in the dynamic light scattering measurement. The structural elements maintained the dispersion state without forming larger aggregates during most water evaporation processes and finally reorganized into film as the water was removed.

The other possible method is the methanolic solution casting method, featuring rapid removal of methanol from a heterogeneous solution. Although the fact that the derivatives are insoluble in methanol had seemed to be a drawback, this method unexpectedly formed thin films from a solution containing products **2** (DS0.03)–**8** (DS0.64); only product **1** (DS0.01) turned into a white solid (Fig. 9i). A dispersion of products **2** (DS0.03) and **3** (DS0.06) formed a fragmented film upon methanol evaporation (Fig. 9j,

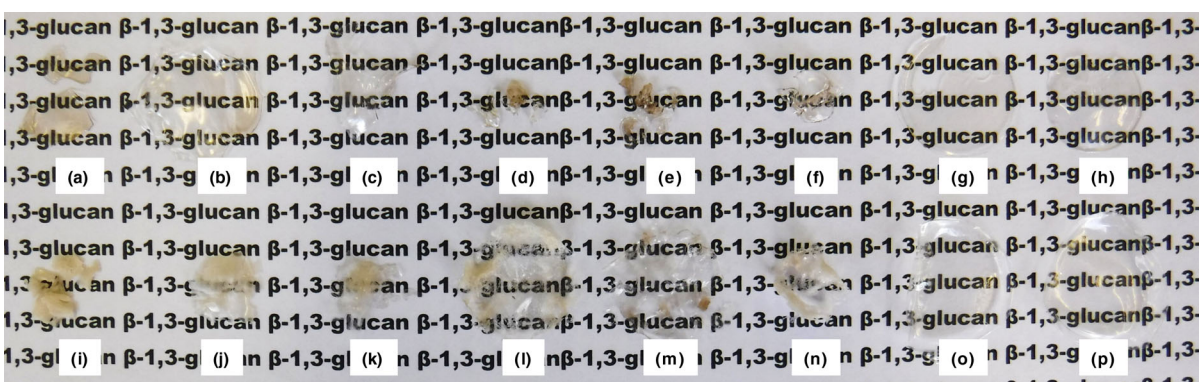

Fig. 9 Photographs of aqueous solution cast films of 2-hydroxy-3-trimethylammoniopropyl paramylons: **a 1** (DS0.01), **b 2** (DS0.03), **c 3** (DS0.06), **d 4** (DS0.07), **e 5** (DS0.11), **f 6** (DS0.16), **g 7** (DS0.31), and **h 8** (DS0.64); ones of methanolic solution cast films: **i 1** (DS0.01), **j 2** (DS0.03), **k 3** (DS0.06), **l 4** (DS0.07), **m 5** (DS0.11), **n 6** (DS0.16), **o 7** (DS0.31), and **p 8** (DS0.64)

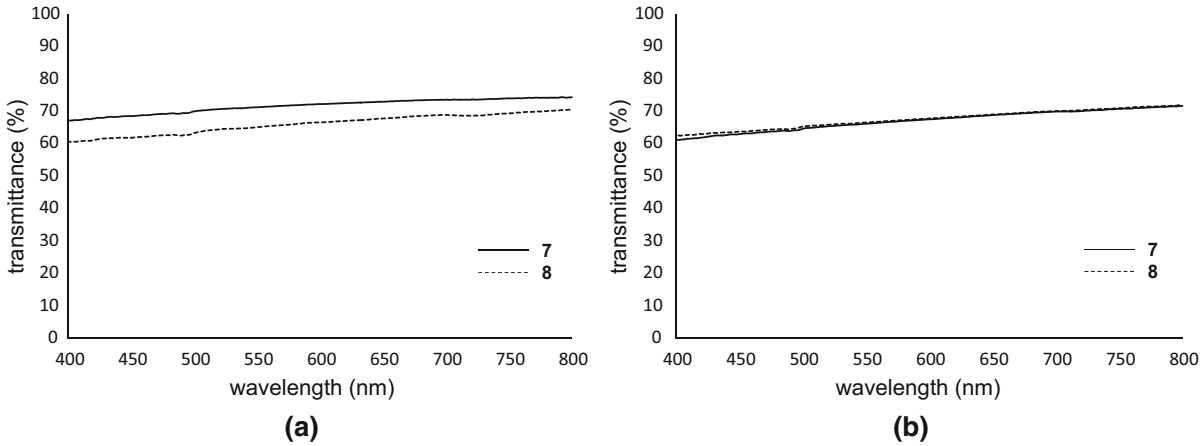

Fig. 10 Light transmittance spectra of thin films of 2-hydroxy-3-trimethylammoniopropyl paramylons [**7** (DS0.31) and **8** (DS0.64)] prepared by **a** aqueous solution casting and **b** methanolic solution casting

k). A convoluted-shaped transparent cast film formed from products **4** (DS0.07)–**6** (DS0.16) (Fig. 9l–n). Of particular note was that a distinctly outlined, round-shaped transparent thin film formed from products **7** (DS0.31) and **8** (DS0.64) (Fig. 9o, p). These results indicate that cationic paramylon derivatives with higher DS_{hta} are capable of reorganizing themselves into a film upon being dispersed in methanol. Although the detailed mechanism of the formation remains to be elucidated, our results indicate that these derivatives are inherently dispersible in methanol.

Evaluation of optical property and surface morphology of thin films made from 2-hydroxy-3-trimethylammoniopropyl paramylons

As described in the previous section, it is likely that cationic paramylon derivatives with DS_{hta} greater than 0.31 (i.e., products **7** (DS0.31) and **8** (DS0.64) exhibit high film formability. To gain further insight into this possibility, the properties of films made from products **7** (DS0.31) and **8** (DS0.64) were examined using visible spectroscopy and SPM. A specific question to answer was whether film transparency and surface roughness depended on the solvent species used for the solution casting. Thus, the films made from products **7** (DS0.31) and **8** (DS0.64) using the aqueous and methanolic solution casting methods were examined.

First, the film transparency was examined by visible spectroscopy. As shown in Fig. 10, the transmittance of the films made from products **7** (DS0.31) and **8** (DS0.64) ranged approximately from 60 to 70% in the visible light region. That is, although the product **7** (DS0.31) film prepared by aqueous solution casting showed slightly higher transmittance, there was little difference among them. Given the insolubility of the derivatives in methanol, products **7** (DS0.31) and **8** (DS0.64) apparently have unique dispersion and aggregation characteristics by which they rearrange themselves from a coagulated solid state into a transparent film state without being fully dissolved in methanol.

Next, to examine the dependence of surface roughness on the solvent species used in the casting procedure, SPM was conducted on two thin films made from product **7** (DS0.31) prepared by aqueous and methanolic solution casting. Figure 11a shows a surface image of a square area $\sim$ 1 μm on a side and a cross-sectional one of the film prepared by aqueous solution casting. The height difference in the cross-sectional image is $\sim$ 7.5 nm over an approximately 1-μm distance. The surface roughness of the observed area, represented by the arithmetic average roughness (R_a), was 1.142 nm. Figure 11b shows images of the film prepared by methanolic solution casting. The height difference was $\sim$ 2.6 nm, and R_a was 4.343 nm, indicating that there was no substantial difference in the surface roughness in the 1-μm-square area between these two films. Figure 11b also shows that the methanol soluble part and the insoluble one for product **7** (DS0.31) were possibly separated when the film was prepared using methanolic solution casting.

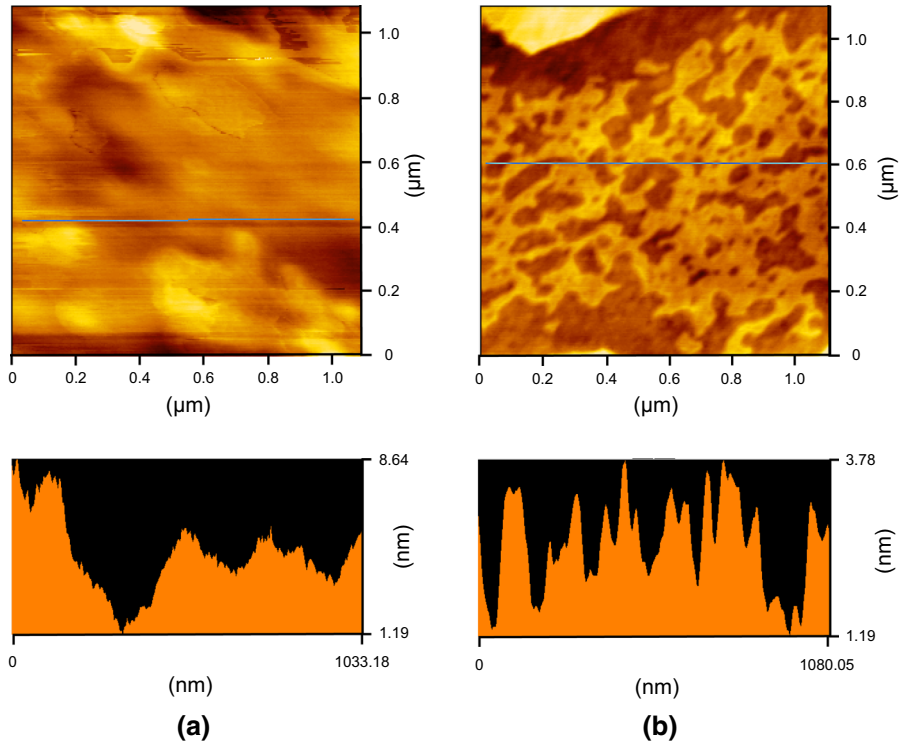

Fig. 11 Scanning probe microscopic images of surface and cross-section of thin films made from 2-hydroxy-3-trimethylammoniopropyl paramylons [**7** (DS0.31)] prepared by **a** aqueous solution casting and **b** methanolic solution casting

Conclusion

We examined the dependence of the dissolution, dispersion, and oriented aggregation characteristics of 2-hydroxy-3-trimethylammoniopropyl paramylons on the degree of substitution of the cationic functional group. Cationic paramylon derivatives with a medium degree of substitution (0.07–0.16) exhibited spontaneous nanofiber formation in aqueous solution simply upon the freeze-dried products being mechanically stirred in water. Cationic paramylon derivatives with a degree of substitution higher than 0.31 did not exhibit a similar spontaneous aggregation characteristic in aqueous media because of their high water solubility; instead, they formed a distinctly outlined, transparent thin film featuring nanometer-level flatness using the solution casting methods. Although the derivatives with a degree of substitution less than 0.06 were less or not dispersible in water and methanol, they were capable of forming a thin film from a heterogeneous aqueous and methanolic solution. Studies currently in progress are aimed at developing organic materials on the basis of the nanofiber/film formability. The results will be reported in due course.

Acknowledgments The authors are grateful to KOBELCO Eco-Solutions Co. Ltd. for providing the paramylon. They are also grateful to Dr. Kijima (AIST) for technical assistance in obtaining the WAXD data.

References

Barsanti L, Vismara R, Passarelli V, Gualtieri P (2001) Paramylon (beta-1,3-glucan) content in wild type and WZSL mutant of *Euglena gracilis.* Effects of growth conditions. J Appl Phycol 13:59–65

Bluhm TL, Sarko A (1977) Triple helical structure of Lentinan, a linear beta-(1-]3)-D-glucan. Can J Chem 55:293–299. https://doi.org/10.1139/V77-044

Booy FP, Chanzy H, Boudet A (1981) An electron-diffraction study of paramylon storage granules from *Euglena gracilis*. J Microsc 121:133–140

Chuah CT, Sarko A, Deslandes Y, Marchessault RH (1983) Packing analysis of carbohydrates and polysaccharides. 14. Triple-helical crystalline-structure of curdlan and paramylon hydrates. Macromolecules 16:1375–1382. https://doi.org/10.1021/Ma00242a020

Clarke AE, Stone BA (1960) Structure of the paramylon from *Euglena gracilis*. Biochim Biophys Acta 44:161–163

Deslandes Y, Marchessault RH, Sarko A (1980) Packing analysis of carbohydrates and polysaccharides. 13. Triple-helical structure of (1-]3)-beta-D-glucan. Macromolecules 13:1466–1471. https://doi.org/10.1021/Ma60078a020

Edgar KJ, Buchanan CM, Debenham JS, Rundquist PA, Seiler BD, Shelton MC, Tindall D (2001) Advances in cellulose ester performance and application. Prog Polym Sci 26: 1605–1688. https://doi.org/10.1016/s0079-6700(01)00027-2

Ifuku S, Saimoto H (2012) Chitin nanofibers: preparations, modifications, and applications. Nanoscale 4:3308–3318. https://doi.org/10.1039/c2nr30383c

Ifuku S, Ikuta A, Egusa M, Kaminaka H, Izawa H, Morimoto M, Saimoto H (2013) Preparation of high-strength transparent chitosan film reinforced with surface-deacetylated chitin nanofibers. Carbohyd Polym 98:1198–1202. https://doi.org/10.1016/j.carbpol.2013.07.033

Isogai A, Saito T, Fukuzumi H (2011) TEMPO-oxidized cellulose nanofibers. Nanoscale 3:71–85. https://doi.org/10.1039/c0nr00583e

Iwatake A, Nogi M, Yano H (2008) Cellulose nanofiber-reinforced polylactic acid. Compos Sci Technol 68:2103–2106. https://doi.org/10.1016/j.compscitech.2008.03.006

Kobayashi K, Kimura S, Togawa E, Wada M, Kuga S (2010) Crystal transition of paramylon with dehydration and hydration. Carbohyd Polym 80:491–497

Marchessault RH, Deslandes Y (1979) Fine-structure of (1-]3)-beta-D-glucans—curdlan and paramylon. Carbohyd Res 75:231–242

Marubayashi H, Yukinaka K, Enomoto-Rogers Y, Takemura A, Iwata T (2014) Curdlan ester derivatives: synthesis, structure, and properties. Carbohyd Polym 103:427–433. https://doi.org/10.1016/j.carbpol.2013.12.015

Nichifor M, Stanciu MC, Simionescu BC (2010) New cationic hydrophilic and amphiphilic polysaccharides synthesized by one pot procedure. Carbohyd Polym 82:965–975. https://doi.org/10.1016/j.carbpol.2010.06.027

Puanglek S, Kimura S, Iwata T (2017) Thermal and mechanical properties of tailor-made unbranched alpha-1,3-glucan esters with various carboxylic acid chain length. Carbohyd Polym 169:245–254. https://doi.org/10.1016/j.carbpol.2017.04.015

Sakagami H et al (1989) Chemical modification potentiates paramylon induction of antimicrobial activity. In Vivo 3:243–248

Santek B, Friehs K, Lotz M, Flaschel E (2012) Production of paramylon, a ss-1,3-glucan, by heterotrophic growth of *Euglena gracilis* on potato liquor in fed-batch and repeated-batch mode of cultivation. Eng Life Sci 12:89–94. https://doi.org/10.1002/elsc.201100025

Shibakami M (2017) Thickening and water-absorbing agent made from euglenoid polysaccharide. Carbohyd Polym 173:451–464. https://doi.org/10.1016/j.carbpol.2017.06.025

Shibakami M, Sohma M (2017) Synthesis and thermal properties of paramylon mixed esters and optical, mechanical, and crystal properties of their hot-pressed films. Carbohyd Polym 155:416–424. https://doi.org/10.1016/j.carbpol.2016.08.093

Shibakami M, Sohma M, Hayashi M (2012) Fabrication of doughnut-shaped particles from spheroidal paramylon granules of *Euglena gracilis* using acetylation reaction. Carbohyd Polym 87:452–456. https://doi.org/10.1016/j.carbpol.2011.08.012

Shibakami M, Tsubouchi G, Nakamura M, Hayashi M (2013a) Polysaccharide nanofiber made from euglenoid alga. Carbohyd Polym 93:499–505. https://doi.org/10.1016/j.carbpol.2012.12.040

Shibakami M, Tsubouchi G, Nakamura M, Hayashi M (2013b) Preparation of carboxylic acid-bearing polysaccharide nanofiber made from euglenoid beta-1,3-glucans. Carbohyd Polym 98:95–101. https://doi.org/10.1016/j.carbpol.2013.05.026

Shibakami M, Tsubouchi G, Hayashi M (2014) Thermoplasticization of euglenoid beta-1,3-glucans by mixed esterification. Carbohyd Polym 105:90–96. https://doi.org/10.1016/j.carbpol.2014.01.053

Shibakami M, Tsubouchi G, Sohma M, Hayashi M (2015) One-pot synthesis of thermoplastic mixed paramylon esters using trifluoroacetic anhydride. Carbohydr Polym 119:1–7. https://doi.org/10.1016/j.carbpol.2014.11.036

Shibakami M, Tsubouchi G, Sohma M, Hayashi M (2016) Synthesis of nanofiber-formable carboxymethylated Euglena-derived β-1,3-glucan. Carbohyd Polym 152:468–478. https://doi.org/10.1016/j.carbpol.2016.06.100

Suflet DM, Popescu I, Pelin IM, Nicolescu A, Hitruc G (2015) Cationic curdlan: synthesis, characterization and application of quaternary ammonium salts of curdlan. Carbohyd Polym 123:396–405. https://doi.org/10.1016/j.carbpol.2015.01.050

Teramoto Y, Yoshioka M, Shiraishi N, Nishio Y (2002) Plasticization of cellulose diacetate by graft copolymerization of epsilon-caprolactone and lactic acid. J Appl Polym Sci 84:2621–2628. https://doi.org/10.1002/app.10430

Tezuka Y (1993) 13C NMR determination of the distribution of two ester substituents in cellulose acetate butyrate. Carbohyd Res 241:285–290. https://doi.org/10.1016/0008-6215(93)80117-W

Tezuka Y, Tsuchiya Y (1995) Determination of substituent distribution in cellulose acetate by means of a 13C NMR study on its propanoated derivative. Carbohyd Res 273:83–91. https://doi.org/10.1016/0008-6215(95)00107-5

Tezuka Y, Imai K, Oshima M, K-i I (1991) 13C-N.m.r. structural study on an enteric pharmaceutical coating cellulose derivative having ether and ester substituents. Carbohyd Res 222:255–259. https://doi.org/10.1016/0008-6215(91)89024-A